X-641-73-167
PREPRINT

X- 70421

ANALYSES OF THE GAMMA-RAY PULSE-HEIGHT SPECTRA FROM THE LUNAR SURFACE

JACOB I. TROMBKA

JUNE 1973

GSFC —— GODDARD SPACE FLIGHT CENTER ——
GREENBELT, MARYLAND

ANALYSES OF THE GAMMA-RAY PULSE-HEIGHT SPECTRA

FROM THE LUNAR SURFACE

Jacob I. Trombka
Laboratory For Space Physics

June 1973

GODDARD SPACE FLIGHT CENTER
Greenbelt, Maryland

CONTENTS

ANALYSES OF THE GAMMA-RAY PULSE-HEIGHT SPECTRA FROM THE LUNAR SURFACE

INTRODUCTION

Scintillation spectrometers are used to measure the characteristic gamma-ray emission spectrum from the moon. The measured pulse-height spectrum is not identical with the true photon spectrum, which is of significance in terms of geochemical interpretation. Furthermore, the lunar gamma-ray emission spectrum can be considered to consist of two components: a component made of discrete energies that can be used directly to infer elemental surface composition and a component characterized by a distribution continuous in energy. This latter component can be associated with such processes as Compton scatter of gamma rays and Bremsstrahlung in the lunar surface. Surface composition cannot be directly inferred from this component. There are a number of other background interferences, such as gamma-ray induced and natural radioactivity in the spacecraft, diffuse gamma-ray background, and spallation effects. In terms of the analytic method to be described in this section, we will only consider the analytic method for obtaining the elemental composition from the observed lunar surface spectrum. The problem is twofold. First, one must infer the true photon spectrum from the measured pulse-height spectrum and, second, determine the magnitude of the discrete and continuous components of the emission spectrum.

We will first consider the method of inferring photon spectra from an analysis of the measured pulse-height spectrum. The term "pulse-height" is used to describe the spectrum because the detector output is usually an analog voltage or current signal which is digitized by using a multichannel pulse-height analyzer. The pulse-height spectrum is a measure of the interaction between the incident gamma ray and the detector. We can describe this interaction process as follows:

$$Y(V) = \int_0^{E_{max}} T(E)S(E,V)dE \tag{1}$$

where $Y(V)$ =   measured pulse-height or interaction spectrum as a function of pulse-height V

$T(E)$ =   differential energy photon spectrum as a function of E

$S(E,V)$ =   detector interaction function reflecting the mechanisms of converting photons of energy, E, into a pulse-height signal, V, at the output of the detector.

The problem is to infer $T(E)$ from $Y(V)$ and a knowledge of the function $S(E,V)$.

We now consider the shape of S(E, V) and its variation with energy. The pulse-height spectrum obtained when monoenergetic gamma rays are detected using a scintillation system is never a line. Its shape is determined by gamma-ray energy and source detector configuration. The shapes of these monoenergetic pulse-height spectra are primarily determined by the relative magnitude of the photoelectric absorption, Compton scattering, and pair-production cross sections and the losses and statistical fluctuations that characterize the crystal, light collection, and photomultiplier system.

One can determine the shape of the interaction spectrum by determining the amount of kinetic energy imparted to an electron by the particular gamma-ray interaction.

Let us examine the case where photoelectric absorption predominates and Compton scattering and pair production are thought to be negligible. In this process the kinetic energy imparted to a secondary electron is equal to the energy of the gamma ray minus the electron binding energy. This binding energy can be reclaimed in terms of the scintillation process by the absorption of the X-rays produced after photoelectric absorption. There is also the possibility that the X-rays may escape the crystal without being absorbed. The pulse-height distribution caused by photoelectric absorption is characterized by two regions: the region of total absorption (the photopeak) and the region of total absorption minus X-ray escape energy (the escape peak). This distribution spreading, plus the Gaussian spreading previously discussed, yields a pulse-height spectrum similar to that shown in Figure 1, the 0.298 MeV line.

When Compton scattering becomes an important energy-loss mechanism, another region, the so-called Compton continuum, is observed in the pulse-height spectrum. In terms of the scintillation process, all the energy lost in scattering will be given up to the electron as kinetic energy. The gamma ray may lose part of its energy to the crystal; furthermore, after suffering a Compton collision or a number of Compton collisions, it may suffer a photoelectric absorption and lose its remaining energy. Thus, the gamma ray either loses all of its energy in the crystal or loses part of its energy in the crystal while the remainder of the ray escapes the crystal at a diminished energy. (See Figure 1, the 0.826 MeV/line.)

At energies higher than 2 MeV, pair production becomes appreciable. In Figure 1, one observes two false "photopeaks" in the pulse-height spectrum for an energy of 2.41 MeV incident upon the 8- by 8-cm (3- by 3-in) NaI(Tl) detector. The pulse heights of the three peaks, in order of increasing pulse height, are caused by:

- Pair production with escape of both annihilation quanta

- Pair production with the absorption of one annihilation quantum

- Pair production with absorption of both annihilation quanta and total absorption by photoelectric effect or any combination of other effects leading to total absorption

In addition to the photopeak, the iodine X-ray escape peak, the Compton continuum, and the pair escape peaks, there are a number of other regions characteristic of experimentally determined monoenergetic pulse-height spectra:

- The multiple Compton scattering region—Because of such scattering from materials surrounding the source and crystal, thus degrading the primary energy, there is a continuous distribution of gamma rays incident upon the crystal with energies less than the maximum energy.

- Annihilation radiation from the surroundings—Positrons emitted from the source may annihilate the surrounding material. Some of the 0.51-MeV gamma rays produced in such a manner will reach the crystal, and a pulse-height spectrum characteristic of 0.51-MeV gamma rays will be superimposed on the monoenergetic pulse-height spectrum.

- Coincidence distribution—If two gamma rays interact with the crystal during a time shorter than the decay time of the light produced in the scintillation process, a pulse will appear whose height is proportional to the sum of energies lost to the crystal by both interacting gamma rays.

Because the interaction time of both single and multiple interactions is shorter than the decay time of the light in the crystal, a single gamma ray interacting with the crystal produces only one pulse. The magnitude of the pulse height is affected by the type or number of interactions for a given gamma ray. Thus, if the above-mentioned coincidence effects are negligible, the measured monoenergetic pulse-height spectrum can be considered as a distribution of the probability of energy loss as a function of energy for the given gamma-ray energy and geometrical configuration. In addition, the shape of the monoenergetic pulse-height distribution depends on the source detector geometry.

The functions S(E, V) can either be experimentally determined or theoretically calculated. Radioactive sources were available to study this energy dependence experimentally up to 3 MeV, and neutron capture methods were used to study crystal response up to 10 MeV.[2] The lower and higher experimentally determined energy-response functions were then calculated using stochastic (Monte Carlo) techniques and found to be in good agreement.[2,3] We therefore feel that the response function can be calculated theoretically for any energy needed in the analysis considered in the following discussion. The three pulse-height spectra shown in Figure 1 have been produced by the stochastic calculation technique.

Now that we have a method for calculating S(E, V), we can consider methods for determining T(E) in Equation (1). The analysis of gamma-ray pulse-height spectra in this particular spectral region must be accomplished by numerical methods because we cannot yet perform this inverse transform analytically. The integral in Equation (1) can be written as a sum of discrete components. T(E) is not a discrete distribution in energy, but a continuous energy distribution. The method for obtaining T(E) is based on a theorem in sampling theory[4] and on the fact that there is a finite energy resolution of the detection system. If a distribution has no oscillatory component with a frequency greater than f_{max}, then the Shannon sampling theorem asserts that samples at discrete points not farther apart than $0.5\text{-}f_{max}$, describe the original function exactly. The original function may be reconstructed from the samples.[5] Thus, Equation (1) can be written as

$$Y_i = \sum_j T_j S_{ij} \tag{2}$$

where Y_i is the measurement of Y(V) in channel or pulse height i, T_j is the total number of gamma rays in energy group ΔE_j about E_j and S_{ij} is the value of the j-th standard spectrum in channel i. The S_{ij} components are the response of an NaI(Tl) detector to an incident monoenergetic gamma ray.

In applying Shannon's sampling theorem to the analysis of spectra obtained with NaI(Tl) crystals, sampling components S_{ij} are chosen so that their separation energy is no greater than the half-width at half-maximum of their photopeaks. Further, the integral in Equation (1) is a sum of discrete energy components that describe an energy interval ΔE about a given E; the energy intervals between the ΔE samples are less than the half-width at half-maximum of the photopeak for the function S(E, V).[4,6] Thus the approximation formula, Equation (2), is obtained. Equation (2) is now in a form where a valid numerical transformation can be obtained using techniques derived from the analysis of variance. The details of this derivation can be found in Reference 5. Using

the least-squares principle, the method requires that

$$M = \sum_i \omega_i (Y_i - \sum_j T_j S_{ij})^2 \qquad (3)$$

be a minimum, where ω_i is the statistical weight corresponding to the measurement of Y_i on channel i and $\omega_i = 1/\sigma_i^2$, where γ_i^2 is the variance of the count in channel i. The partial derivatives of M are taken with respect to T in order to determine the minimum. The solution in matrix form is given by Equation (4)

$$T = (\tilde{S}\omega S)^{-1} \tilde{S}\omega Y \qquad (4)$$

where T is a best estimate of the differential energy photon spectrum, S is an m x n matrix describing the discrete set of detector response functions (library functions) using the selection rule derived here, $\tilde{S}$ is the transposition of S, ω is a square diagonal matrix of the weighting functions, and Y is a vector describing the pulse-height spectrum. A detailed description of the calculated method and computer program is found in Reference 6.

At this point we are now able to transform from pulse-height space to photon space. Our major problem occurs because we have a mixture of discrete lines and continuum. This problem is further complicated in the determinations of the inverse matrix $(S \omega \tilde{S})^{-1}$. One obtains oscillations in the solution due to interference between the components of the S matrix. These oscillations become most pronounced in the vicinity of discrete lines. Methods have been developed for damping these oscillations. These methods consist of trying to obtain a description of the continuous component using the transposition from pulse height to energy space [Equation (4)], eliminating all possible discrete lines and points on either side of these lines where oscillations occur, and finding the best fit of a power law distribution to the remaining points. Therefore, we assume that the continuum can be approximated by the function

$$T_c = AE^{-n} \qquad (5)$$

where T_c is the differential energy spectrum for the continuum component of the incident flux, A is the amplitude, and n is the power law to be determined by fitting those points on characterizing the continuous distribution.

Once T_c is determined, the pulse-height spectrum of the T_c background distribution can be obtained using Equation (2). This pulse-height spectrum can be subtracted from the measured spectrum, and the pulse-height distribution of

the discrete component is obtained. This can then be converted to a photon spectrum. The geochemical information is then inferred from this final distribution.

USE OF THE ANALYTICAL METHOD

An example of the analytical method may be of help in understanding its application. Using the methods considered in Reference 7, the discrete line gamma-ray emission spectrum from the lunar surface for a given composition can be obtained. An average lunar surface composition for the major element composition was assumed and is indicated in Table 1. The expected photon flux is also shown. Using stochastic methods, a pulse-height spectrum due to the discrete lines observed at the orbital attitude with a 7- by 7-cm (2.75- by 2.75-in) NaI(Tl) detector is calculated. The detector resolution for 0.661 MeV is assumed to be 8.5 percent. We then assumed that the continuum spectrum was of the form $T_c \propto E^{-1.3}$. From the Soviet Luna-10 data,[7] we estimated that the continuous distribution was about 85 percent of the total observed flux from the lunar surface. Finally, it was assumed that the spectrum was obtained over a 200-min integration time. The calculated spectrum is shown in Figure 2. The spectrum is further degraded to correspond with the actual measurement by allowing for random fluctuations due to counting statistics in each channel. The spectrum is divided into 511 channels. Thus both crystal size and pulse-height analyzer correspond to the system used during the Apollo mission.

The pulse-height spectrum is transformed to a photon spectrum using a 118-component monoenergetic library. The results are displayed on a log-log plot in Figure 3. The oscillation, especially around discrete energies and at high energies, can be seen. These oscillation and discrete energy components are eliminated. Seventeen points remain to characterize the continuous distribution (the points circled). A least-square fit is performed assuming a power law dependence [Equation (5)]. Both the magnitude A and power n are determined. For this particular case it was found that A = 0.062 and n = 1.33, only 2.3 percent from the value assumed in the calculation. The calculated power law distribution of the continuum is shown in Figure 3. Using the values of A and n obtained from the least-square fit, the shape and magnitude of the pulse-height spectrum of the continuous spectrum can be obtained and is shown in Figure 4. This component is subtracted from the spectrum shown in Figure 2, and an estimate of the discrete line spectrum is obtained and shown in Figure 5.

At this point, pulse-height spectra characteristic of the elemental reaction components are used for the library. For example, the pulse-height spectrum for natural emission from thorium is shown in Figure 6, and the pulse-height spectrum expected from the $O(n, n, \gamma)$ reaction is shown in Figure 7. The

6

reaction considered, forming a 15 component library, is shown in Table 1. Using this library, the elemental photon flux and elemental composition can be obtained by matrix inversion [Equation (4)].

The results of the analysis of the discrete pulse-height spectra are shown in Table 1. Both photon flux and weight fraction of the particular element are indicated. These results are compared with the values actually used in the calculation. If our assumptions about the continuum and discrete energy spectra are correct, our capabilities for obtaining qualitative and quantitative elemental analysis from the measured gamma-ray spectra can be evaluated. The errors indicated in the table are associated with counting statistics and background subtraction. Our ability to determine the natural radioactive elements thorium, uranium, and potassium should be limited only by counting statistics. The results agree well with the true values. The induced activities of $Mg(n, n, \gamma)$, $Fe(n, n, \gamma)$, $Si(n, n, \gamma)$, and $Ca(n, \gamma)$ can be used to determine the elemental weight fraction of magnesium, iron, silicon, and calcium. For the counting times indicated, the statistical error in determining the elemental weight fraction for titanium and aluminum from the $Ti(n, n, \gamma)$ and $Al(n, \gamma)$ reactions will be rather large. There is one other major source of error in the determination of the elemental weight fraction. This error can be attributed to interference between various spectral shapes; that is, the inability to resolve elemental components separately. An analysis of the covariance between various elemental components making up the pulse-height spectra of the libraries used in the analysis of the discrete spectra has been carried out and the percent interference between various components calculated. The method of calculation is described in Reference 7. The higher the percent of interference, the more difficult it is to resolve the particular reactions. Our laboratory experience indicates that interferences greater than 20 percent cause trouble in interpretation. Table 2 indicates the interference percentages greater than 20 between the various library components used in the analysis of the elemental reaction pulse-height spectra. For example, one finds that the $Fe(n, \gamma)$ spectrum strongly interferes with the $O(n, n, \gamma)$, $Si(n, n, \gamma)$, and $Al(n, \gamma)$ spectra. Thus one would be hard put to use these results to determine Fe concentration, for example. The poor results for oxygen, titanium, and aluminum may also be explained by this interference problem.

The procedure for analyzing the measured pulse-height spectra described should allow us to perform analysis of the Apollo-15 and -16 gamma-ray spectrometer data. Both qualitative and quantitative results should be obtained, and both accuracy and precision of results in terms of counting statistics, background subtraction, and spectral interference can be obtained.

7
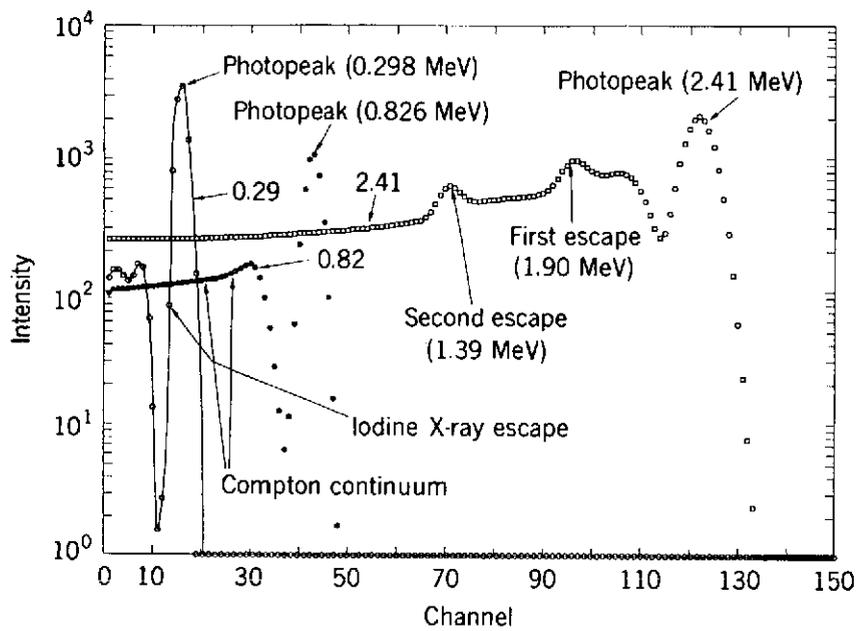
Figure 1. Pulse–height spectrum of monoenergetic gamma rays incident upon an 8– by 8–cm NaI(Tl) detector (~19 keV per channel).
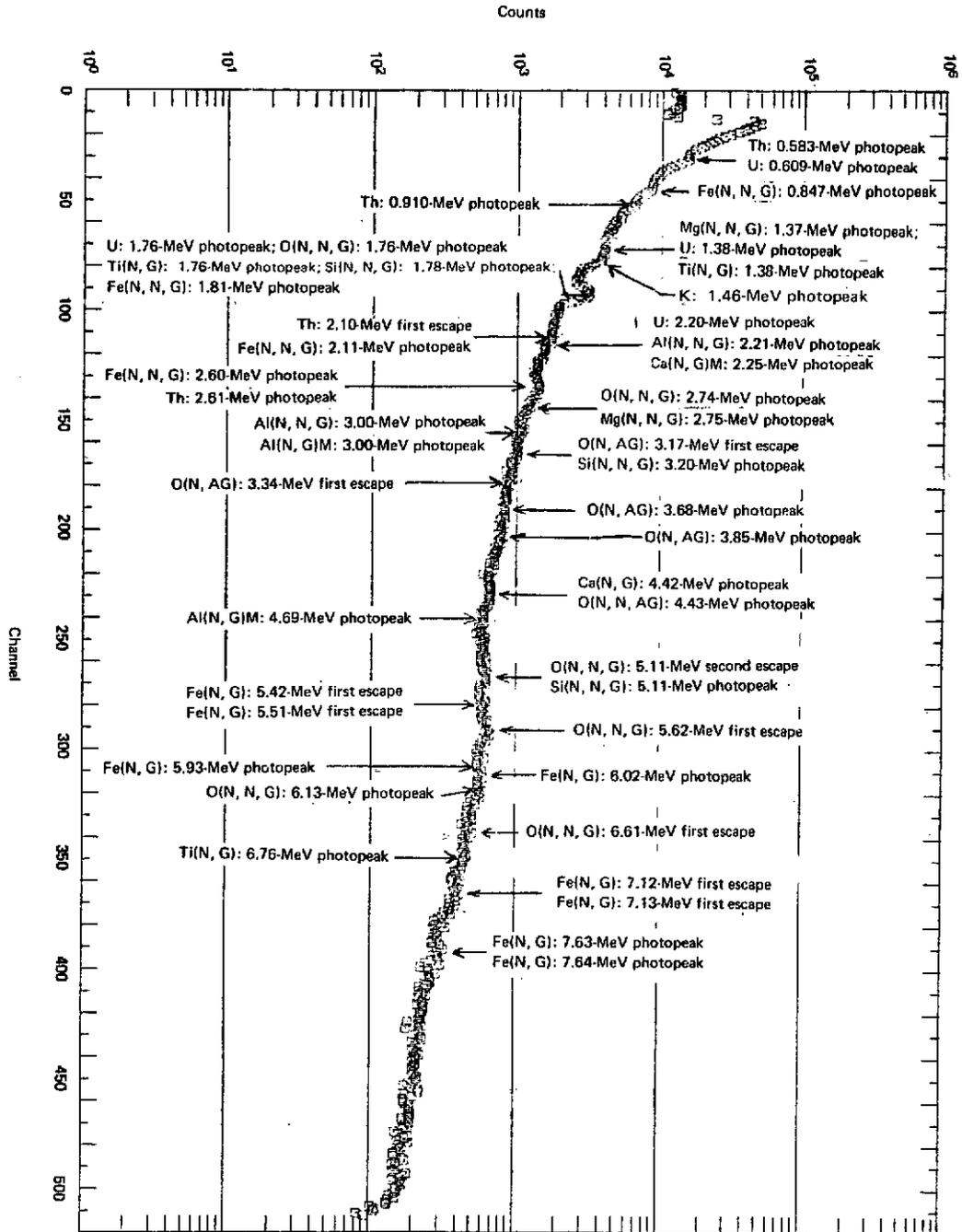
Figure 2. Calculated lunar pulse-height spectrum 7- by 7-cm NaI(Tl) crystal;~19keV per channel; 200 min integration time).
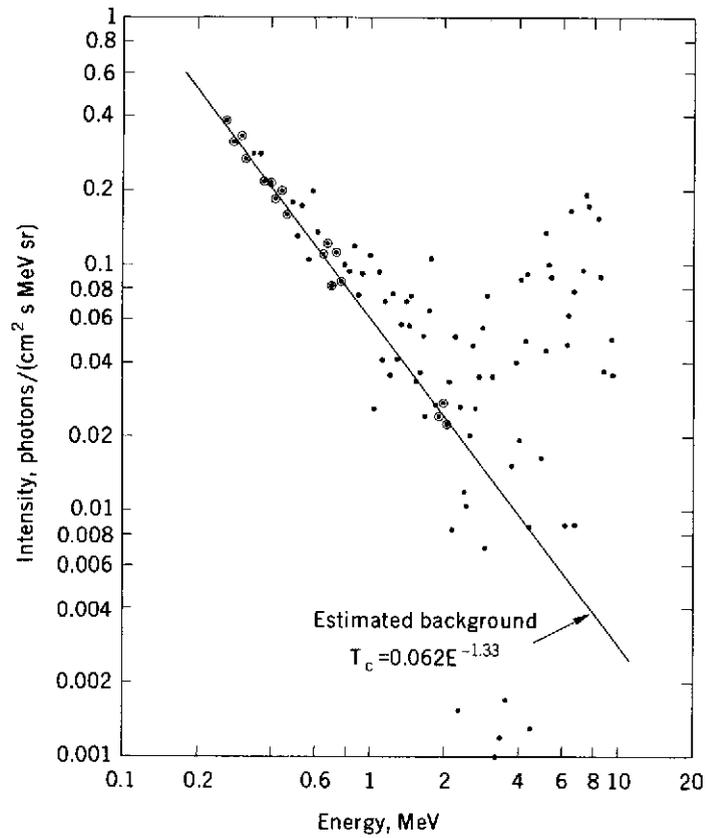
Figure 3. Lunar photon spectrum inferred from lunar
pulse-height spectrum.
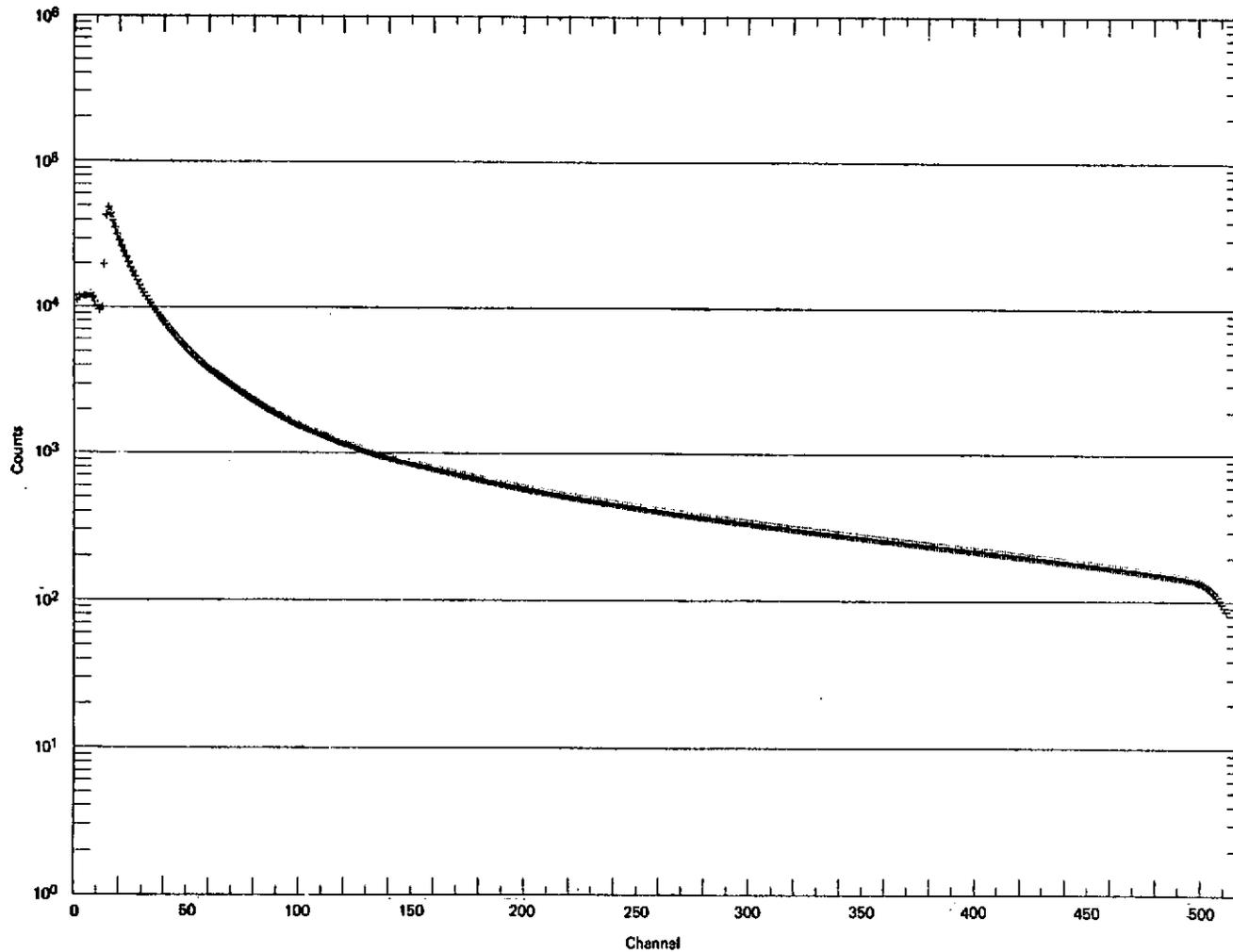
Figure 4. Pulse-height spectrum of continuous distribution assuming a power-law spectrum $E^{-1.33}$ (7- by 7-cm NaI(Tl) crystal;~19 keV per channel).

Counts

Channel

Th: 0.239-MeV photopeak
Th: 0.337-MeV photopeak
Ti(N, G): 0.341-MeV photopeak
U: 0.352-MeV photopeak
Th: 0.583-MeV photopeak
U: 0.609-MeV photopeak
Fe(N, N, G): 0.847-MeV photopeak
Th: 0.910-MeV photopeak
U: 1.12-MeV photopeak
Fe(N, N, G): 1.24-MeV photopeak
Mg(N, N, G): 1.37-MeV photopeak
K: 1.46-MeV photopeak
U: 1.38-MeV photopeak
Ti(N, G): 1.38-MeV photopeak
U: 1.75-MeV photopeak
O(N, N, G): 1.76-MeV photopeak
Ti(N, G): 1.76-MeV photopeak
Si(N, N, G): 1.78-MeV photopeak
Fe(N, N, G): 1.81-MeV photopeak
Th: 2.10-MeV first escape
U: 2.20-MeV photopeak
Al(N, N, G): 2.21-MeV photopeak
Fe(N, N, G): 2.11-MeV photopeak
O(N, N, G): 2.23-MeV first escape; Mg(N, N, G): 2.24-MeV first escape
Fe(N, N, G): 2.60-MeV photopeak; Th: 2.61-MeV photopeak
O(N, N, G): 2.74-MeV photopeak; Mg(N, N, G): 2.75-MeV photopeak
Si(N, N, G): 2.83-MeV photopeak
Al(N, N, G): 3.00-MeV photopeak
Al(N, G)M: 3.00-MeV photopeak
O(N, AG): 3.17-MeV first escape
Si(N, N, G): 3.20-MeV photopeak
O(N, AG): 3.34-MeV first escape
Fe(N, N, G): 3.60-MeV photopeak
O(N, AG): 3.68-MeV photopeak
O(N, AG): 3.85-MeV photopeak
Al(N, G)M: 4.00-MeV photopeak
O(N, N, AG): 4.43-MeV photopeak
Al(N, G)M: 4.69-MeV photopeak
O(N, N, G): 5.11-MeV second escape
Si(N, N, G): 5.11-MeV photopeak
Fe(N, G): 5.42-MeV first escape
Fe(N, G): 5.51-MeV first escape
Ca(N, G): 5.40-MeV second escape
O(N, N, G): 5.62-MeV first escape
Ca(N, G): 5.91-MeV first escape
Fe(N, G): 5.93-MeV photopeak
Fe(N, G): 6.02-MeV photopeak
O(N, N, G): 6.13-MeV photopeak
Ca(N, G): 6.42-MeV photopeak
O(N, N, G): 6.61-MeV first escape
Ti(N, G): 6.76-MeV photopeak
Fe(N, G): 7.12-MeV first escape
Fe(N, G): 7.13-MeV first escape
Fe(N, G): 7.63-MeV photopeak
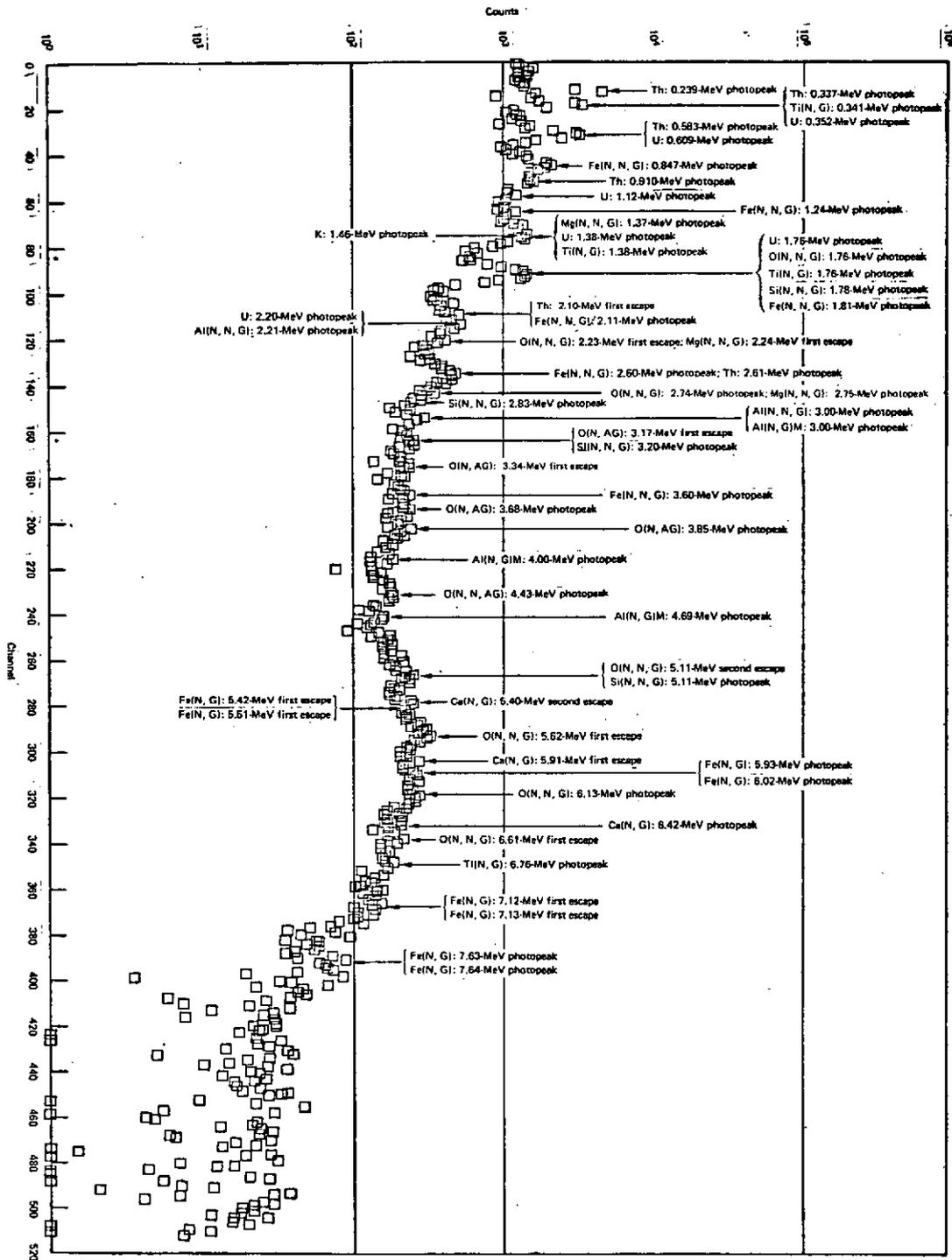Fe(N, G): 7.64-MeV photopeak

Figure 5. Pulse-height spectrum of the discrete line in the lunar surface emission spectrum (7- by 7-cm NaI(Tl) crystal; ~19 keV per channel).
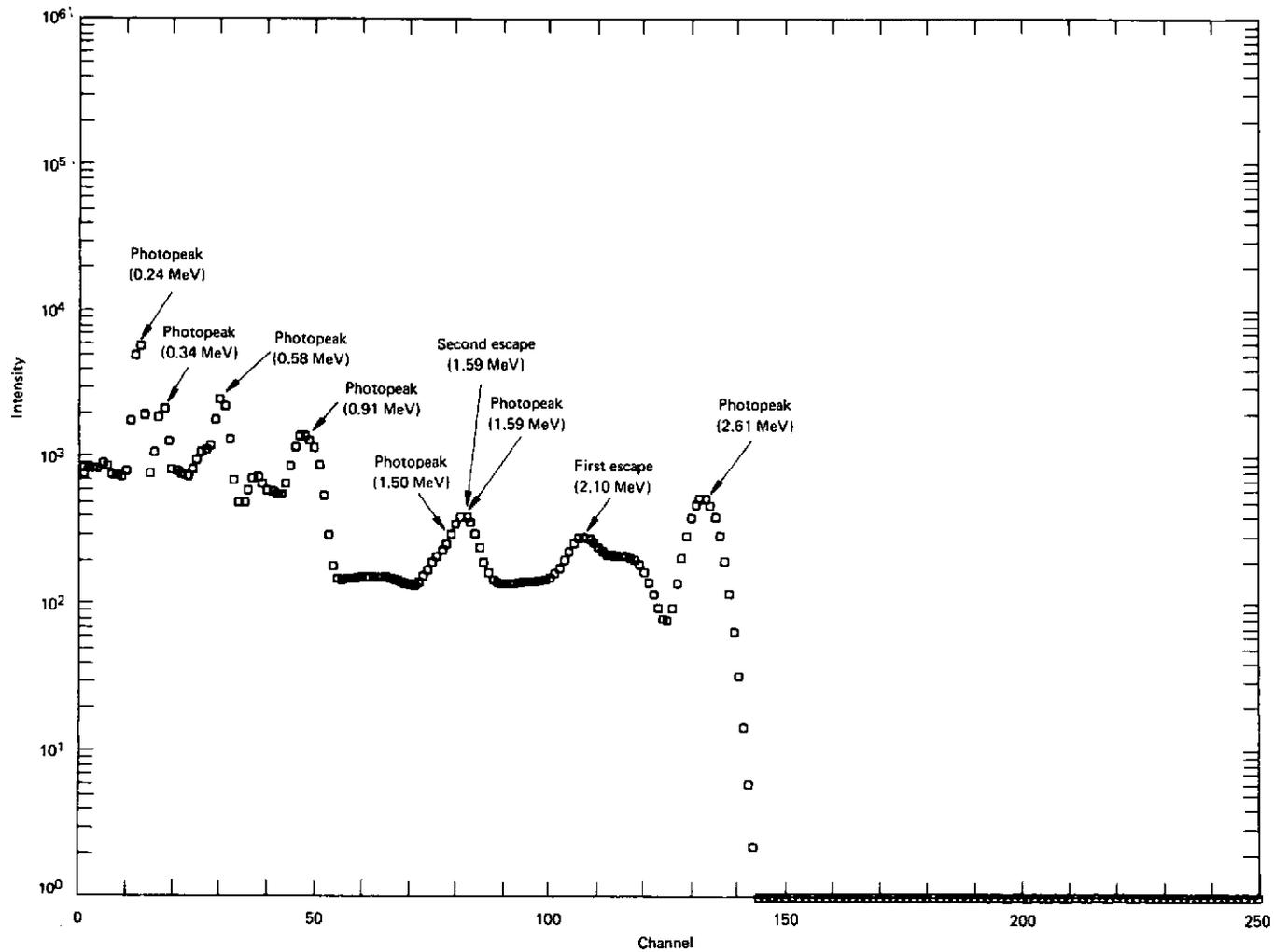
12

Figure 6. Calculated pulse-height spectrum for thorium (7- by 7-cm NaI(Tl) spectrum;~19 keV per channel).
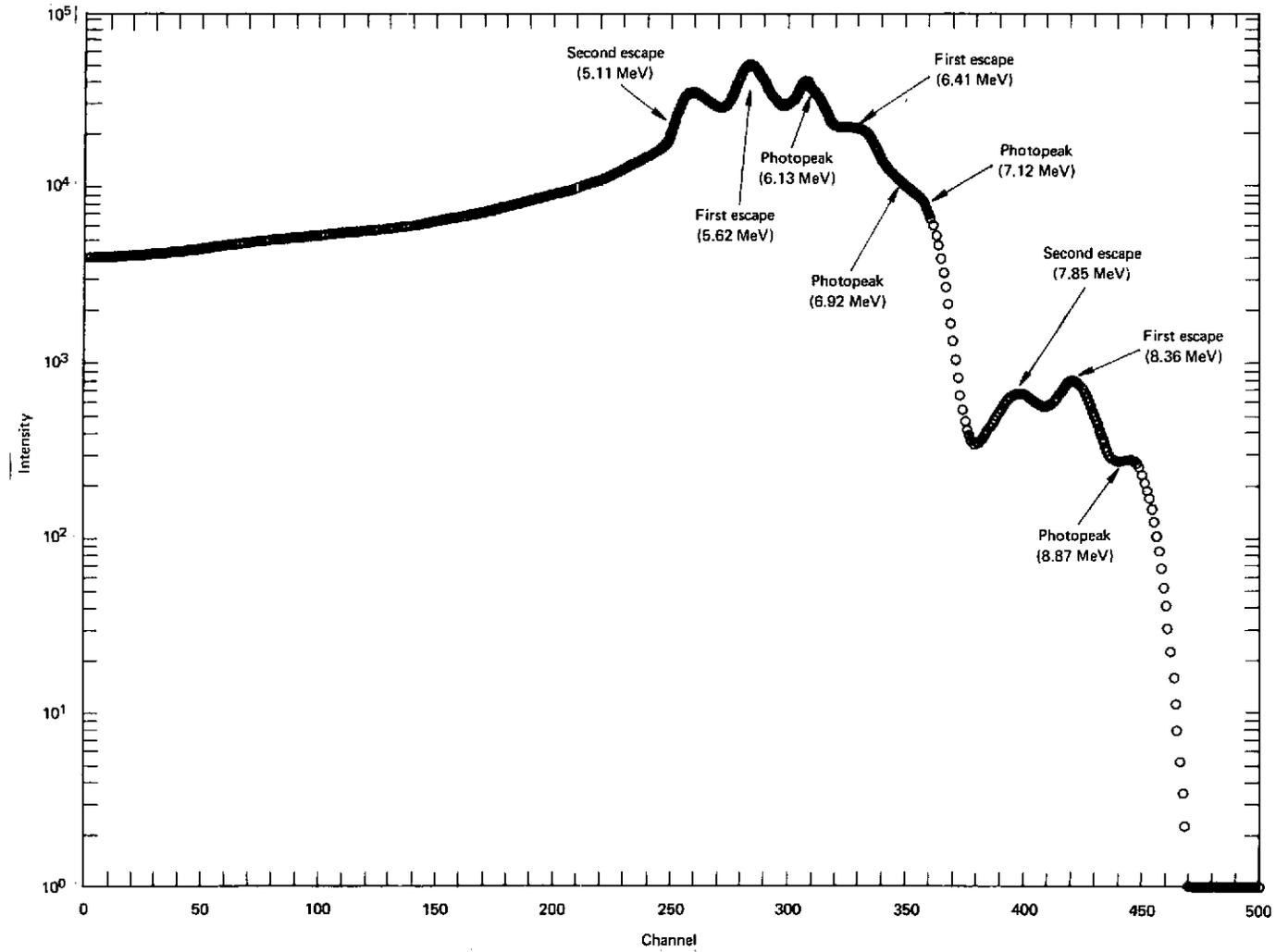
13

Figure 7. Pulse-height spectrum for the O(n, n, γ.) reaction (7- by 7-cm
NaI(Tl) crystal;~19 keV per channel).

14

Table 1

Theoretical and Calculated Weight Fraction and Fluxes for Average Lunar Composition

Element	Theoretical		Calculated	
	Weight fraction	Flux, photons/(cm^2 s sr)	Weight fraction	Flux, photons/(cm^2 s sr)
Th	2.1×10^{-6}	7.84×10^{-3}	$2.11 \pm 0.14 \times 10^{-6}$	$7.89 \times 10^{-3} \pm 0.53 \times 10^{-3}$
Mg(n, n, γ)	0.05	1.23×10^{-3}	0.060 ± 0.012	$1.47 \times 10^{-3} \pm 0.30 \times 10^{-3}$
U	0.55×10^{-6}	4.84×10^{-3}	0.53 ± 0.04	$4.64 \times 10^{-3} \pm 0.39 \times 10^{-3}$
O(n, n, γ)	0.42	6.13×10^{-3}	0.49 ± 0.05	$7.22 \times 10^{-3} \pm 0.73 \times 10^{-3}$
Al(n, n, γ)	0.10	2.84×10^{-3}	0.15 ± 0.02	$4.25 \times 10^{-3} \pm 0.64 \times 10^{-3}$
Fe(n, n, γ)	0.10	2.07×10^{-3}	0.10 ± 0.01	$2.11 \times 10^{-3} \pm 0.23 \times 10^{-3}$
Si(n, n, γ)	0.21	5.10×10^{-3}	0.21 ± 0.03	$5.08 \times 10^{-3} \pm 0.68 \times 10^{-3}$
Ca(n, n, γ)	0.09	4.46×10^{-4}	0.22 ± 0.07	$1.07 \times 10^{-3} \pm 0.36 \times 10^{-3}$
Ti(n, n, γ)	0.015	1.49×10^{-4}	0.010 ± 0.026	$9.71 \times 10^{-5} \pm 2.62 \times 10^{-5}$
Al(n, γ)	0.10	6.49×10^{-4}	0.15 ± 0.17	$9.74 \times 10^{-4} \pm 10.98 \times 10^{-4}$
Si(n, γ)	0.21	1.18×10^{-3}	0.35 ± 0.08	$1.96 \times 10^{-3} \pm 0.44 \times 10^{-3}$
Ca(n, γ)	0.09	7.80×10^{-4}	0.11 ± 0.05	$9.65 \times 10^{-4} \pm 4.40 \times 10^{-4}$
Ti(n, γ)	0.015	1.75×10^{-3}	0.011 ± 0.005	$1.28 \times 10^{-3} \pm 0.57 \times 10^{-3}$
Fe(n, γ)	0.20	2.88×10^{-3}	0.14 ± 0.02	$3.89 \times 10^{-3} \pm 0.54 \times 10^{-3}$
K–40	1150×10^{-6}	2.20×10^{-3}	$1168 \pm 92 \times 10^{-6}$	$2.24 \times 10^{-3} \pm 0.18 \times 10^{-3}$

Table 2

Percent Interference Between Library Components

	Th	Mg(n, n, γ)	U	O(n, n, γ)	Al(n, n, γ)	Fe(n, n, γ)	Si(n, n, γ)	Ca(n, n, γ)	Ti(n, n, γ)	Al(n, γ)	Si(n, γ)	Ca(n, γ)	Ti(n, γ)	Fe(n, γ)	K-40
Th	100		20.2												
M(n. n, γ)		100		21.0					29.9						
U	20.2		100												
O(n, n, γ)		21.0		100				31.5					51.2	22.4	
Al(n, n, γ)					100										
Fe(n, n, γ)						100									
Si(n, n, γ)							100			73.6				56.7	
Ca(n, n, γ)				31.5				100						21.5	
Ti(n, n, γ)									100						
Al(n, γ)							73.6			100				79.2	
Si(n, γ)											100				
Ca(n, γ)												100			
Ti(n, γ)		29.9		51.2									100		
Fe(n, γ)				22.4			56.7	21.5		79.2				100	
K-40															100

REFERENCES

1. P. R. Bell. "The Scintillation Process." Beta and Gamma Ray Spectroscopy. Kai Siagbaum, ed. North Holland Pub. Co. Amsterdam. 1955.

2. J. I. Trombka, E. Eller, G. A. Osswald, M. J. Berger, and S. M. Seltzer. "252 Cf Neutron Induced Radioactive Capture Gamma Rays for High Energy Detector Calibration." Neutron Sources and Applications, III. USAEC Report CONF. -710402. 1971. p. 43.

3. S. M. Seltzer and M. J. Berger. "Response of NaI Detectors to High-Energy Gamma Rays." Amer. Nucl. Soc. Transactions, 14-1. 1971. pp. 124-125.

4. D. A. Linden. "Discussion of Sampling Theorem." Proc. IRE, 47. 1959.

5. J. I. Trombka, F. Seuftle, and R. Schmadebeck. "Neutron Radioactive Capture Methods for Surface Elemental Analysis." Nuc. Instr. Meth., 87. 1970. pp. 37-41.

6. J. I. Trombka and R. L. Schmadebeck. "A Numerical Least-Square Method for Resolving Complex Pulse-Height Spectra." NASA SP-3044 1968.

7. A. P. Vinogradov, I. A. Surkov, G. M. Chernov, and F. F. Kirnogov. "Measurements of Gamma Radiation of the Moon's Surface by the Cosmic Station Luna 10." Geochemistry, 8. U. I. Vernadsky Institute of Geochemistry and Analytical Chemistry, Moscow, USSR. 1966. p. 891.